The Journal of Neuroscience, December 1995, 15(12): 8000–8010

Cellular Processing of Temporal Information in Medial Vestibular Nucleus Neurons

Sascha du Lac and Stephen G. Lisberger

Department of Physiology and W. M. Keck Foundation Center for Integrative Neuroscience, University of California at San Francisco, San Francisco, California 94143

Quantitative descriptions of the cellular transformations from behaviorally relevant inputs into temporal patterns of firing are crucial for understanding information processing in systems of neurons and for incorporating biological properties of neurons into models of the neural control of behavior. To understand how neurons that mediate vestibulo-ocular behavior transform their inputs into temporal patterns of firing, we examined responses of medial vestibular nucleus (MVN) neurons to current injected intracellularly. MVN neurons recorded from avian brain slices fired spontaneously. Sinusoidal modulation of input current produced precisely sinusoidal modulation of firing rate. The transformation between input current and firing rate was remarkably linear: firing rate scaled linearly as a function of current amplitude, and the responses to steps of input current were predicted accurately from the linear superposition of responses to sinusoidal modulation of input current. Over the physiological range of head movement frequencies, from 0.1 to 10 Hz, peak-to-peak modulation of firing rate was relatively constant or increased slightly in most neurons. In contrast, when hyperpolarizing current was used to keep neurons below threshold for action potentials, the frequency response of the membrane potential behaved like a low-pass filter. These results imply that the membrane conductances that are active when MVN neurons fire compensate for the low-pass characteristics of the membrane to allow faithful transmission of high frequency head movement signals.

[Key words: spike generation, vestibulo-ocular reflex, firing rate, temporal filtering, medial vestibular nucleus, frequency response]

A combination of network and cellular mechanisms transform sensory information into behavioral commands. Understanding the neural basis of behavior therefore requires quantitative descriptions of how both systems of neurons and individual neurons process incoming information. Because it has been studied so thoroughly in intact animals, the vestibulo-ocular reflex (VOR) provides an excellent behavioral system for understanding the relative contributions of network and cellular mechanisms to the generation of behavior.

To generate the VOR, central vestibular neurons transform time-varying head movement information into precise patterns of firing in extraocular motoneurons. The transformation from sensory signals into motor outputs has three important features. First, incoming head movement signals must be passed with high fidelity over a wide frequency range, from about 0.1 to 10 Hz, and the highest frequency signals must be amplified (Keller, 1978). Second, head velocity signals must be mathematically integrated to produce the eye position related firing of extraocular motoneurons (Skavenski and Robinson, 1973). Finally, because the behavioral response to head movement exhibits both short- and long-term plasticity (Ito et al., 1974; Gonshor and Melvill-Jones, 1976; Melvill-Jones, 1977; Collewijn and Grootendorst, 1978; Miles and Eighmy, 1980; Wallman et al., 1982; Schairer and Bennett, 1986; Snyder and King, 1992), the processing of head movement information must be modifiable.

It has been traditional to assume that information processing in the VOR results from network properties and that individual neurons themselves either pass incoming signals unaltered or attenuate and delay responses at high frequencies. However, individual neurons contain a variety of membrane and synaptic properties that could contribute to the processing of vestibulo-ocular information and that undoubtedly contribute to behavioral learning. The goal of this article is to determine how cellular mechanisms of single vestibular neurons contribute to information processing in the VOR. The head movement signals that guide the VOR enter the brain via the vestibular nerve and are subjected to the first stage of central processing in the vestibular nuclei. Much is already known how neurons in the medial vestibular nucleus (MVN) fire during vestibulo-ocular behavior (Fuchs and Kimm, 1975; Lisberger and Miles, 1980; Chubb et al., 1984; Tomlinson and Robinson, 1984; McCrea et al., 1987a,b; Ohgaki et al., 1988; McFarland and Fuchs, 1992; Scudder and Fuchs, 1992; Cullen et al., 1993; Cullen and McCrea, 1993; Lisberger et al., 1994a,b), so we have selected these neurons for study with intracellular recordings in *in vitro* brainstem slices.

In the vestibular and oculomotor systems, most neurons fire action potentials spontaneously, and information appears to be encoded in modulations of firing rate. We consider the cellular processing of firing rate information as having three broad stages. First, the firing of presynaptic neurons is transformed by synaptic machinery into current at the postsynaptic neuronal dendrites (and/or soma). Second, passive cable properties and active dendritic conductances filter the synaptic current. Finally,

Received June 5, 1995; revised Aug. 3, 1995; accepted Aug. 7, 1995.

We thank E. J. Chichilnisky for many valuable discussions and E. J. Chichilnisky, David Heeger, David Perkel, and Peter Schwindt for their comments on previous versions of the manuscript. Supported by NIH Grants EY11027 to S.dL. and EY03878 to S.G.L., and by a Development Award from McKnight Neuroscience Endowment Foundation to S.G.L.

Correspondence should be addressed to Sascha du Lac, Department of Physiology, Box 0444, UCSF, San Francisco, CA 94143-0444.

filtered current at the soma and axon hillock gets transformed into temporal patterns of action potentials via a process called *spike generation.*

In the present study, we investigate the contributions of spike generation in MVN neurons to temporal information processing. To determine how MVN neurons transform behaviorally relevant information into a firing rate code, we measured firing rate responses to intracellularly injected current that was modulated sinusoidally over the physiological range of head movement frequencies. To determine how the membrane conductances that are active during spike generation shape the responses to temporally modulated inputs, we compared the frequency response of the spike generator with that of the membrane below spike threshold. Our results demonstrate that MVN neurons transform inputs into firing rate in a precise and linear fashion over the behaviorally relevant range of input frequencies. Over a large range of firing rates, the responses to high frequency inputs are strong, indicating that active membrane conductances compensate for the passive filtering properties of the membrane, enabling MVN neurons to transmit high frequency head movement information.

Materials and Methods

Brainstem slices containing the medial vestibular nucleus were prepared from 2–12 d old chicks. The slice preparation has been described in detail previously (du Lac and Lisberger 1995). In brief, chicks were anesthetized with ketamine (5 mg), decapitated, and the brainstem was dissected from the skull under Ringer's bubbled with carbogen (95% O_2 and 5% CO_2). Transverse slices containing the medial vestibular nucleus were cut on a vibratome (Campden) at a thickness of 450–500 μM. Slices were incubated in carbogenated Ringer's at room temperature for at least 1 hr before recordings began. Carbogenated Ringer's had a final pH of 7.4 and contained (in mM): NaCl, 130; KCl, 3; $MgSO_4$, 1.5; $NaHCO_3$, 26; $CaCl_2$, 2.5; NaH_2PO_4, 1.75; and dextrose, 10.

Recordings were made in a submersion-type chamber through which carbogenated ringer, warmed to 31–33°C flowed at 4–5 ml/min. Microelectrodes were filled with 3 M KCl or 3 M KAc and ranged from 50 to 100 MΩ in resistance; we found no differences in the properties of neurons recorded with different electrolytes. Recordings were made with an Axoclamp 2-A (Axon Instruments) in current-clamp mode; the bridge balance was checked and adjusted regularly throughout the course of the experiments. Membrane potential measurements for each neuron were adjusted for any offset in potential following removal of the electrode from the neuron. Signals were filtered at 3 kHz, amplified 50×, and digitized at a sample rate of at least 5 kHz by an 386 IBM-compatible computer.

During the initial 5–10 min after neurons were impaled, the input resistance, spontaneous firing rate, and response to depolarizing current steps often varied. Data collection began after these properties attained stable values. Neurons were injected intracellularly with sinusoidally modulated current; current injection was controlled by the computer. Between 4 and 30 cycles of each of a number of frequencies between 0.1 and 10 Hz were presented. At least 3 sec elapsed between injection of different sinusoidal frequencies. In some neurons, sinusoidal current modulation was superimposed on a steady DC level of current that either depolarized or hyperpolarized the neuron, and frequency responses were collected at two or more different mean firing rates. Following sinusoidal injection, the response to 6–10 steps of depolarizing current were collected. Spontaneous firing rate was measured periodically during the course of the experiment, and the data were discarded if spontaneous rate varied by more than 15% percent of the average rate.

Data analysis

Instantaneous firing rate, $r(t)$, was calculated as the reciprocal of the interval between successive pairs of spikes and assigned to the time, t, of the second spike. This algorithm was chosen to insure that changes in our estimate of firing rate would be related causally to input current, that is, that a measured change in firing rate would not precede the stimulus that caused a change in the interspike interval. Firing rate values were not calculated for times between spikes. Firing rate responses to sinusoidal current injection were fitted with sinusoidal functions of time, $R(t) = a \cdot \sin(2\pi f \cdot t + b) + c$. The parameters of this function, a, f, b, and c, were chosen to minimize the mean squared difference between the actual firing rate, $r(t)$, and predicted sinusoidal firing rate, $R(t)$, at each spike time.

We tested whether firing rate scales linearly as a function of input current amplitude by injecting individual neurons with current modulated sinusoidally at one of a number of frequencies and at a range of amplitudes. To determine whether the peak-to-peak firing rate response scaled linearly with current amplitude, we fitted the firing rate response with a sine wave as above, plotted the amplitude of the best fit sine wave as a function of peak-to-peak current amplitude, and calculated the regression coefficient of the best least squares linear fit of the plotted data.

We tested additivity (superposition) of the transformation from input current into firing rate by comparing a neuron's response to steps of current with that predicted by the same neuron's responses to sinusoidally injected current. Let $Rj(t)$ represent the firing rate, as a function of time, to unit amplitude sinusoidal current injection at j Hz, and let $R'j(t)$ be the response to a square wave modulation of current of unit amplitude, with period j. Denote by $\{R(t)\}$ the modulated component (difference from baseline rate) of the response. Additivity of the modulated components predicts that the $\{R'j(t)\}$ is equal to the Fourier synthesis of the sinusoidal responses:

$$\{R'(t)\} = 4/\pi \cdot [\{R1(t)\} + 1/3 \cdot \{R3(t)\} + 1/5 \cdot \{R5(t)\} \ldots]. \quad (1)$$

This was tested as follows. First, best fitting response gain and phase values for $Rj(t)$ were obtained from each neuron at several input frequencies j from 0.1 to 10 Hz. Next, gain and phase were plotted separately as a function of input frequency, and these plots were fitted with third order polynomials. The polynomials provided good fits to gain and phase as a function of frequency (see Fig. 5). The polynomial fits were then used to interpolate response gain and phase at frequencies j, $3j$, etc., up to a maximum of 10 Hz. The responses $R1(t)$, $R3(t)$, etc., were determined from these gain and phase values, entered into Equation 1, and used to generate a prediction for the firing rate response $R'(t)$. This prediction was regressed against the actual firing rate response to 2–10 repetitions of a step of current of duration $j/2$ (which is half of one cycle of a squarewave stimulus of period j); the quality of the prediction was determined from the correlation coefficients of the linear regression.

Comparisons across neurons. For each neuron, firing rate responses were obtained to sinusoidal current modulated at a fixed amplitude and at frequencies between 0.1 and 10 Hz. The amplitudes of the best fit sine wave to the response at each frequency were then plotted as a function of frequency and fit with a third order polynomial using commercially available software (e.g., Fig. 5*A*,*B*). Response gain was normalized to the value of the polynomial fit at 0.5 Hz. Phase values were not normalized.

Subthreshold measurements. Membrane potential responses to sinusoidal current injection were obtained from neurons that were held below action potential threshold by injection of hyperpolarizing DC current. Membrane potential was fitted with a sinusoidal function of time with the algorithm used to fit sinusoidal firing rate responses. Membrane time constants were obtained from the subthreshold membrane potential response to small hyperpolarizing steps of current. The gain of a first order low-pass filter with time constant T was calculated as $1/\sqrt{(1 + (2\pi fT)^2)}$ where f is the input frequency. The phase, in degrees, was calculated as $180/\pi \cdot \arctan(2\pi fT)$.

Simulations. To investigate the response to sinusoidal input of neuron-like oscillators that convert continuous input into a discrete firing rate code, we constructed two simple models. Both models generate an action potential of fixed height whenever membrane potential crosses a set threshold. Following the action potential, membrane potential is reset to a fixed value below action potential threshold. In the first model, the trajectory of the membrane potential between action potentials is governed by the sum of an intrinsic pacemaking current and injected current, and membrane capacitance, such that $I(\text{total}) = I(\text{inj}) + I(\text{int})$, $I(\text{int}) = g(V_m - V_{eq})$, and $dV_m/dt = I(\text{total})/C$, where $I(\text{int})$ is the intrinsic current, V_{eq} is the equilibrium potential of the intrinsic channel, C is the membrane capacitance, and V_m is the current membrane potential. In the absence of injected current the membrane potential between spikes follows an exponential trajectory and the model fires spontaneously. A given spontaneous firing rate could be achieved with a number of com-

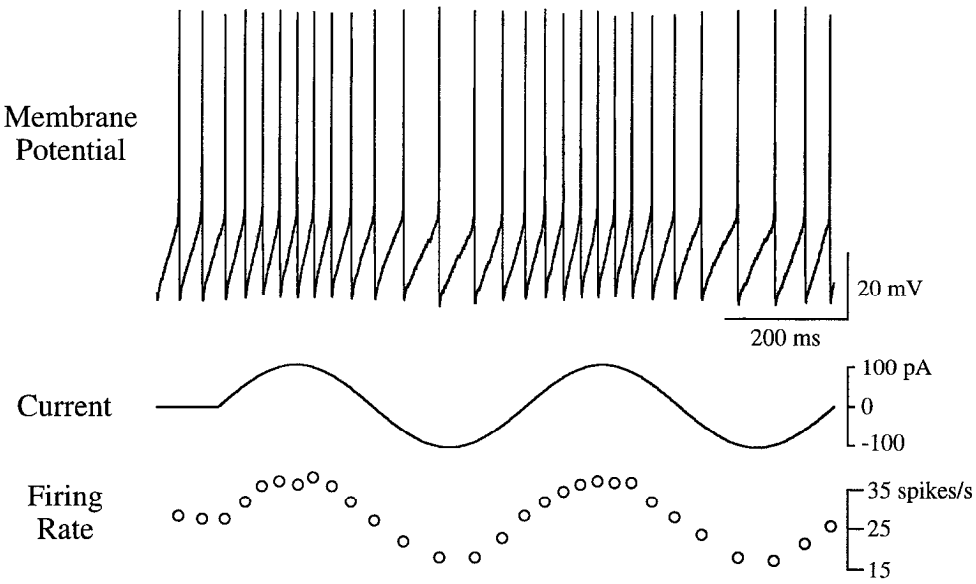

Figure 1. Response of a typical MVN neuron to intracellular injection of sinusoidally modulated current. The *top trace* shows membrane potential as a function of time in response to injection of current, shown in the *middle trace*. The *bottom trace* plots instantaneous firing rate. Sinusoidally alternating depolarization and hyperpolarization of the neuron resulted in alternating increases and decreases in firing rate.

binations of model parameters; however, the qualitative behavior of the model was robust to parameter combination.

The second model contains no intrinsic pacemaking current and therefore does not fire in the absence of injected current. Membrane trajectory between spikes is linear and follows the relationship $dV_m/dt = I(\text{inj})/C$. Injection of constant depolarizing current causes the model to fire at a regular rate determined by the amount of injected current and the model capacitance. The models' firing rate responses to sinusoidally injected current were analyzed with the same algorithms used for real neurons. Response gain was normalized to the gain at 0.5 Hz as described for real neurons; phase was not normalized.

Results

The results represent data from 21 neurons recorded intracellularly in the medial vestibular nucleus (MVN). All of the neurons were spontaneously active, had action potentials that were at least 45 mV in height (from threshold to peak) and rapid afterhyperpolarizations between 10 and 25 mV in depth, and were able to sustain repetitive firing when injected with sustained depolarizing current. Spontaneous firing levels and responses to current injection were stable and consistent over the course of the experiment for each of the neurons in our sample. Intrinsic membrane and firing properties have been described previously and are qualitatively similar both across MVN neurons recorded in avian brain slices and between chicks and mammals (discussed in du Lac and Lisberger 1995).

Responses to sinusoidal current injection

Figure 1 shows a typical example of the response of an MVN neuron to injection of current modulated sinusoidally at 2 cycles/sec ± 100 pA. During the first 100 msec of the trace, no current was injected, and the neuron fired steadily at 27 spikes/sec. Sinusoidal alternation of depolarizing and hyperpolarizing current resulted in alternating increases and decreases in the neuron's instantaneous firing rate. The maximum and minimum firing rates occurred at approximately the same time as the peak depolarizing and hyperpolarizing current, respectively.

Over a wide range of frequencies, sinusoidal modulation of injected current produced sinusoidal modulations in firing rate. Figure 2 shows the responses of a representative neuron to sinusoidal current injection at six different frequencies. The circles in each panel plot instantaneous firing rate as a function of time in response to a particular input frequency, indicated at the top of the panel. The solid line in each panel shows the least-squares sinusoidal fit to the response. The figure illustrates two important points. First, over the range of frequencies from 0.1 to 10 Hz, the modulation of instantaneous firing rate in response to sinusoidal current injection can be well described by a sine wave. Second, the response to current injection is very precise, as indicated by the small amount of scatter of the data around the best fit sine wave.

Sinusoidal current modulation resulted in precise, sinusoidal modulation in firing rate in all of the neurons in our sample. We quantified the responses to sinusoidal current injection by evaluating the correlation coefficient (R^2) of the best fit of the responses to a sine wave. In 21 neurons, over the input frequency ranges from 0.1 to 10 Hz, the mean R^2 value was 0.97 (SD = 0.03). For comparison, the R^2 values of the data shown in Figure 2 ranged between 0.96 and 0.99.

Tests of linearity

The findings that sinusoidal current injection produced precisely sinusoidal modulation in firing rate over a wide range of frequencies suggest that spike generation in vestibular nucleus neurons is linear. We set out to test linearity of the MVN spike generator for two reasons. First, linearity implies that one could predict the pattern of MVN firing in response to any arbitrary input simply by knowing the responses to sinusoidal inputs. Second, linearity of spike generation in MVN neurons has consequences for vestibulo-ocular behavior and implications for the cellular machinery that transforms inputs into action potentials. Two properties—scaling and additivity—must hold for a process to be linear (Bracewell, 1986). That is, the output should scale linearly as a function of the input, and the response to the sum of a number of different inputs should equal the sum of the responses to the individual inputs.

Scaling. To determine whether spike generation in MVN neurons satisfies scaling, we injected individual neurons with sinusoidal input currents at a single frequency and a range of amplitudes and measured the resulting modulation of firing rate. Figure 3 demonstrates this test in a representative neuron. The responses to current modulation at a single frequency of 4 Hz

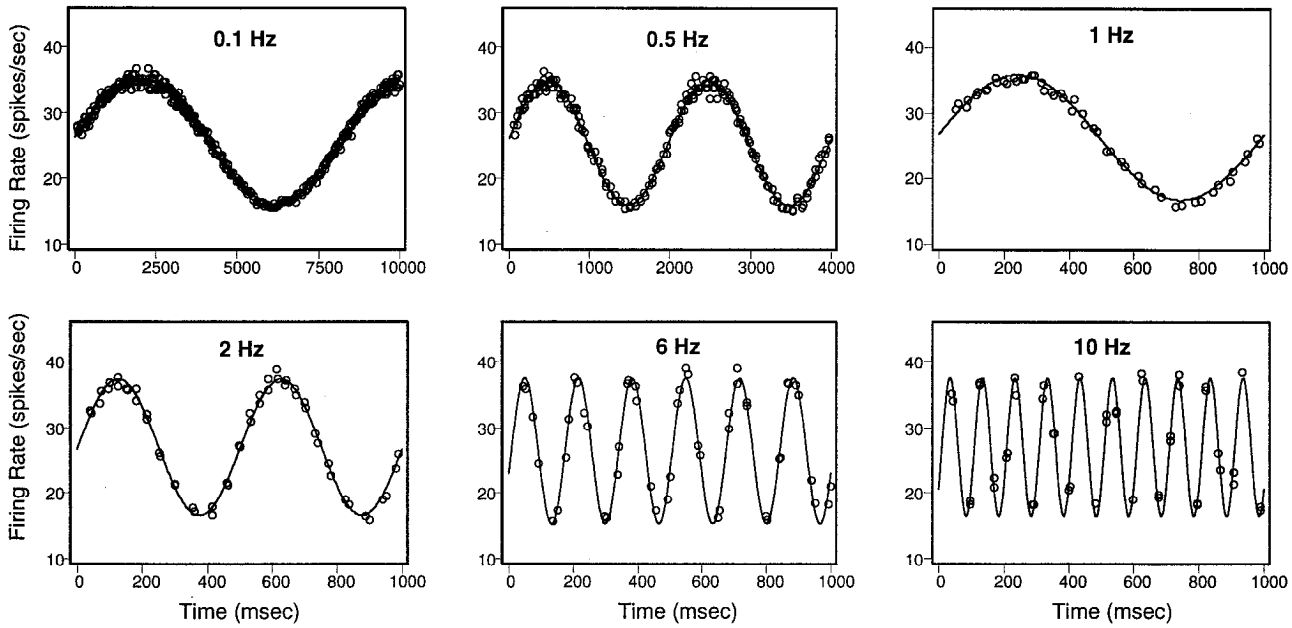

Figure 2. Response of a single MVN neuron to sinusoidal current modulation at six different frequencies. The symbols in each panel show instantaneous firing rate as a function of time in response to intracellularly injected current modulated sinusoidally at the frequency indicated at the top of the panel. Responses to two repetitions of a particular sinusoidal input frequency are shown in each panel. The line indicates the best least squares sinusoidal fit through the data.

and at two different current amplitudes are shown in Figure 3*A*; the solid circles plot instantaneous firing rate as function of time in response to a stimulus with a peak-to-peak amplitude of 100 pA, and the open circles plot the response to a stimulus with a peak-to-peak amplitude of 300 pA. The solid lines indicate sine waves that provided the best fit to the firing rate responses. To determine whether the modulation in firing rate scaled linearly with current amplitude, we obtained the best fit sine wave to the responses of a series of current amplitudes and plotted the peak-to-peak amplitude of the responses as function of the peak-to-peak amplitude of the input current (Fig. 3*B*). The peak-to-peak modulation in firing rate scaled linearly with current amplitude; responses lay close to the regression line. Because the dynamics of the response to a given input should not change as the input

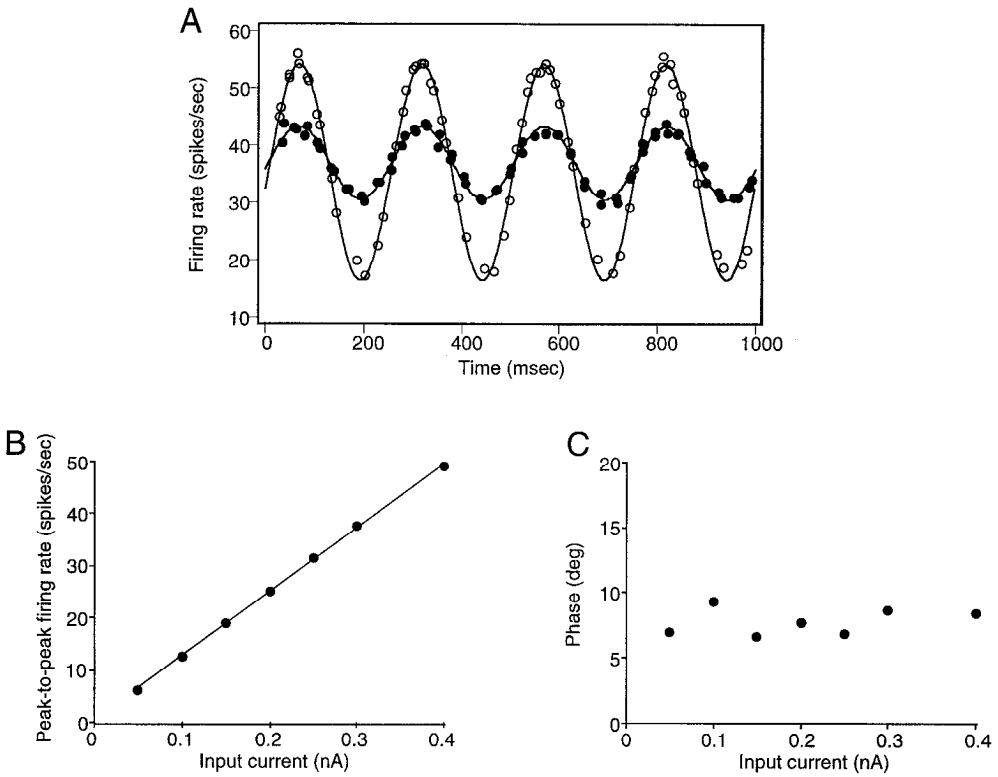

Figure 3. Test of scaling. *A* shows instantaneous firing rate as a function of time in response to injected current modulated sinusoidally at 4 Hz at two different amplitudes in a single neuron. The *solid* and *open symbols* plot the neuron's response to sine waves with peak-to-peak amplitudes of 100 pA and 300 pA, respectively. *Lines through the points* indicate the best least squares sinusoidal fit through the data. *B* plots the peak-to-peak amplitude of the fits to the firing rate responses to sinusoidal current injection as a function of the peak-to-peak amplitude of the injected current. The line indicates the best least squares linear fit through the relationship between current amplitude and peak-to-peak firing rate modulation (R^2 = 0.999). *C* plots the phase of the fits to the firing rate responses to sinusoidal current injection as a function of the phase of the injected current. Positive values indicate that the phase of the response led that of the input.

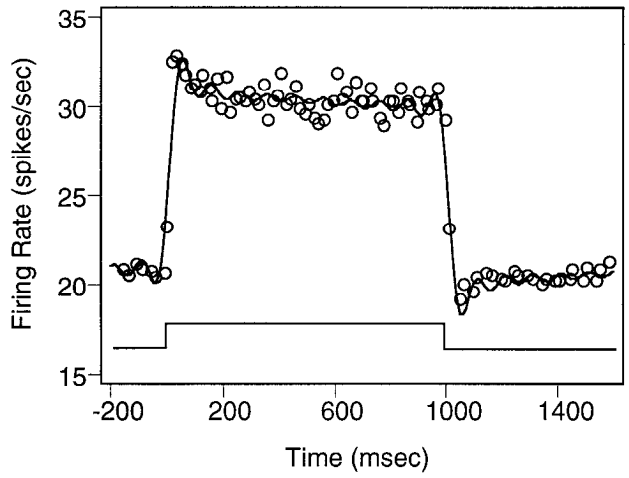

Figure 4. Test of additivity. The *open symbols* indicate instantaneous firing rate, as a function of time, in response to six repetitions of a 200 pA step of current, indicated at bottom. The *line through the points* is the prediction from the Fourier synthesis of the neuron's response to sinusoidal current injection.

is scaled, we also measured the phase shift between the input current and the sine wave that best fitted the data and plotted it as a function of input amplitude. Figure 3*C* demonstrates that the phase of the response did not change with input amplitude.

We tested scaling in a total of eight neurons at three different input frequencies (three neurons at 2 Hz, one at 4 Hz, and four at 8 Hz) and over a range of spontaneous firing rates from 18 to 50 spikes/sec and peak-to-peak modulation amplitudes from 4 to 80 spikes/sec. In each neuron, peak-to-peak firing rate modulation scaled linearly with input amplitude; the correlation coefficients for the best fit line ranged from 0.996 to 0.999. Response phase did not change as a function of input amplitude when the input current was modulated at 2 Hz or 4 Hz. In two of the four neurons tested at 8 Hz, response phase declined by as much as 10° as current amplitude increased. In the other two neurons tested at 8 Hz, response phase was constant across input amplitudes. We conclude that the spike generator in MVN neurons scales its inputs essentially linearly at all frequencies but at high frequencies can produce small changes in response dynamics.

Additivity. To test additivity, we used the approach outlined in the Materials and Methods to compare the actual response to steps of current with that predicted from the Fourier synthesis of the responses to sinusoidally modulated current. Figure 4 shows an example of the comparison in a single neuron. The open circles in Figure 4 show the superimposed firing rate responses to six repetitions of a step of current, indicated by the line at the bottom of the figure. The neuron fired spontaneously at 21 spikes/sec. After the onset of the step, firing rate increased rapidly to a peak of 33 spikes/sec and then decreased to a steady state value of about 31 spikes/sec that was maintained during the step. When the step was turned off, firing rate decreased to a minimum of 18 spikes/sec and then returned to the spontaneous level. The solid line shows the prediction from the Fourier synthesis of the responses to sinusoidal current injection; the close fit (R^2 = 0.97) indicates that spike generation in this neuron satisfies the linear requirement of additivity.

We tested additivity in 12 neurons with mean firing rates between 13 and 68 spikes/sec; the magnitude of the change in firing rate evoked by the steps tested ranged from 6 to 23 spikes/sec. The Fourier synthesis of sinusoidal responses closely predicted firing rate responses to steps of injected current: regression of the predictions on the actual data yielded R^2 values that ranged from 0.83 to 0.98 (median = 0.94). We conclude from this analysis that spike generation in vestibular nucleus neurons satisfies the linear requirement of additivity.

Frequency responses

The findings that spike generation in MVN neurons satisfies both scaling and additivity implies that the spike generator can be thought of as a linear filter. To investigate the filtering properties of the spike generator, we held input current amplitude constant and measured the amplitude and phase of the best sinusoidal fits to the firing rate response to sinusoidal current injection between 0.1 and 10 Hz. Figure 5, *A* and *B*, show the results of this experiment for two different neurons. The symbols in each plot of Figure 5 indicate the actual data; lines drawn through the symbols are 3rd order polynomials that provided the best fit to the data.

The neuron in Figure 5*A* fired spontaneously at 24 spikes/sec. Sinusoidal current injection at a frequency of 0.1 Hz caused a peak-to-peak modulation in the neuron's firing rate of 12.3 spikes/sec (Fig. 5*A1*). As the input frequency increased, the peak-to-peak modulation in firing rate increased slightly, reaching a maximum of 14 spikes/sec at 4 Hz. Firing rate phase with respect to input current phase is shown in Figure 5*A2*. At input frequencies below 0.75 Hz, firing rate phase lagged that of the input by a few degrees. As input frequency increased, firing rate phase led input phase; phase lead increased steadily as a function of input frequency to a maximum of 51° at 10 Hz. The mean firing rate of the neuron shown in Figure 5*A* and of all of the neurons in our sample did not change as a function of sinusoidal input frequency. Figure 5*B* shows data from a different neuron that fired spontaneously at 49 spikes/sec. In this neuron, the peak-to-peak modulation in firing rate increased steadily with input frequency from 10.2 spikes/sec to 13.3 spikes/sec (Fig. 5*B1*). The neuron's response was approximately in phase with injected current at frequencies up to 4 Hz; above this frequency, response phase led that of the input, with phase lead reaching a maximum of 11° at 10 Hz (Fig. 5*B2*).

Effect of mean firing rate. The responses to high input frequencies depended on the neuron's mean firing rate. The effect of mean firing rate is illustrated in Figure 5*C*, which shows the frequency response of a single neuron firing at three different mean rates (spontaneously, at 34 spikes/sec; depolarized with DC current to 49 spikes/sec, and hyperpolarized to 10 spikes/sec). Figure 5*C1* plots response gain, normalized as described in the Materials and Methods. At all three firing rates, gain was essentially constant between input frequencies of 0.1 and 2 Hz. When the neuron fired at a mean rate of 10 spikes/sec, gain dropped rapidly as input frequency increased above 2 Hz. In contrast, when the neuron fired at 34 spikes/sec, gain was relatively constant across all input frequencies. When the neuron fired at 49 spikes/sec, gain increased slightly as input frequency increased between 2 and 10 Hz.

Response phase also depended on mean firing rate. As shown in Figure 5*C2*, the pattern of phase as a function of frequency was similar whether the neuron fired at mean rates of 34 or 49 spikes/sec: firing rate was approximately in phase with input currents at frequencies between 0.1 and 2 Hz, firing rate phase led that of inputs above 2 Hz, and phase lead increased slightly with frequency. In contrast, when the neuron fired at a mean

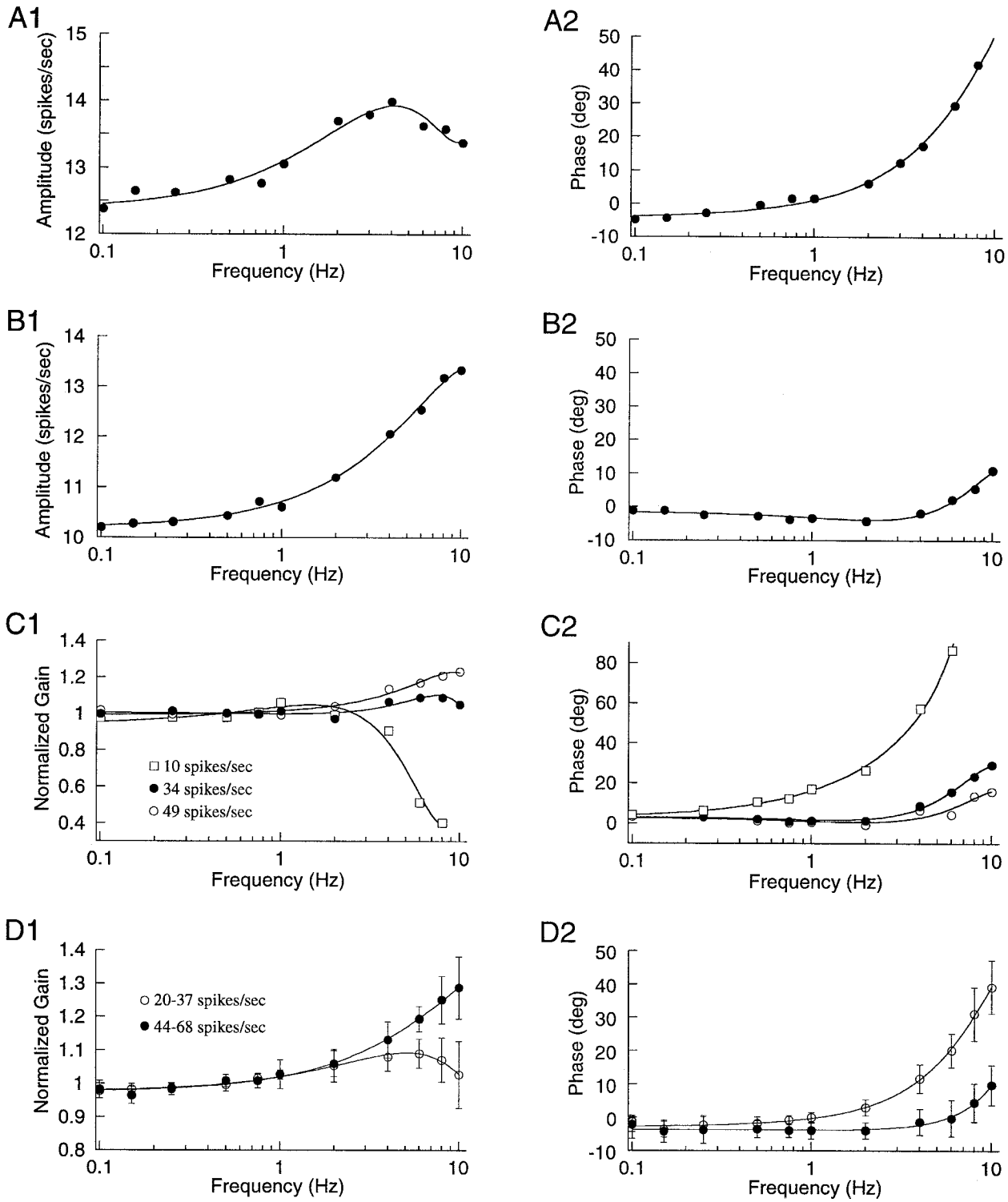

Figure 5. Frequency responses of MVN neurons. *A1* shows the amplitude of the best least squares sinusoidal fit a neuron's response to sinusoidal modulation of current as a function of input frequency. *A2* plots the phase of the best fitting sine wave as a function of input frequency for the same neuron as in *A1*. Positive values of phase indicate that the phase of the response led that of the input. Firing rate in this neuron was modulated around a mean rate of 24 spikes/sec. *B1* and *B2*, same as *A1* and *A2* but for a different neuron in which firing rate was modulated around a mean rate of 49 spikes/sec. *C1* plots the gain of the best fit responses as a function of input frequency to current modulated sinusoidally around three different mean rates: 10 spikes/sec (*squares*), 34 spikes/sec (*solid circles*), and 49 spikes/sec (*open circles*). See Materials and Methods for normalization of response gain. *C2* plots the phase of the best fit responses of the neuron shown in *C1*. *D1* and *2* show the mean gain and phase, respectively, for 13 neurons firing at mean rates between 20 and 37 spikes/sec (*open circles*) and for 9 neurons firing at mean rates between 44 and 68 spikes/sec (*solid circles*). Bars indicate SDs. Lines drawn through the data in each panel are the best (least square) 3rd order polynomial fits of the form: $Y = a + bx + cx^2 + dx^3$. Coefficients for the fits in *D* were as follows. *D1*, 20–37 spikes/sec: $a = 0.97601$; $b = 0.050614$; $c = -0.006371$; $d = 0.00018395$. *D1*, 44–68 spikes/sec: $a = 0.97449$; $b = 0.048132$; $c = -0.0021853$; $d = 5.2670e{-}05$. *D2*, 20–37 spikes/sec: $a = -2.2183$; $b = 2.2566$; $c = 0.41416$; $d = -0.021729$. *D2*, 44–68 spikes/sec: $a = -2.9187$; $b = -0.25813$; $c = 0.14525$; $d = 0.0014006$.

rate of 10 spikes/sec, firing rate phase led that of the input at frequencies greater than 0.5 Hz, and phase lead increased dramatically as a function of frequency.

In our entire sample of neurons, the responses to high frequency inputs depended on mean firing rate. We recorded from four neurons firing at rates less than 20 spikes/sec; in each of them, response gain declined at input frequencies above 2 Hz, and response phase led that of the input by more than 90° at 6–8 Hz. In contrast, Figure 5*D* shows mean gain and phase as a function of frequency for our population of neurons that fired at or above 20 spikes/sec. We have arbitrarily subdivided our sample into two groups, those firing at mean rates between 20 and 37 spikes/sec (n = 13) and those firing at mean rates between 44 and 68 spikes/sec (n = 9). Figure 5*D1* shows that when neurons fired between 20 and 37 spikes/sec, gain tended to be relatively constant between 0.1 and 10 Hz. However, when neurons fired between 44 and 68 spikes/sec, gain tended to increase for input frequencies above 2 Hz. Figure 5*D2* shows that regardless of firing rate, responses were approximately in phase with input frequencies less than about 1 Hz. When neurons fired between 20 and 37 spikes/sec, response phase led that of the input at frequencies greater than 1 Hz, and phase lead increased to a mean of 40° at 10 Hz. When neurons fired at rates between 44 and 68 spikes/sec, phase lead increased much more slowly with frequency, reaching a mean of 10° at 10 Hz. These trends applied both to neurons firing spontaneously and to those in which DC current was injected to elevate spontaneous firing rate.

The variation in gain and phase with mean firing rate indicates that spike generation in MVN neurons is not an entirely linear process. However, the tests of scaling and additivity demonstrate that when the mean firing rate is constant, spike generation acts as a linear filter. To describe quantitatively the linear filtering properties of the MVN spike generator, we fit 3rd order polynomials to the population gain and phase as a function of frequency for neurons firing between 20 and 37 spikes/sec and for those firing between 44 and 68 spikes/sec. Third order polynomials described the population data quite well; the R^2 values for the fits shown in Figures 5*D1* and *2* ranged between 0.988 and 0.999 (the coefficients of the fit are given in the caption to Fig. 5).

Comparison with subthreshold frequency responses. To determine whether the filtering properties of the spike generator differ from those of the neuron's membrane when it is below spike threshold, we hyperpolarized neurons with DC current to a stable membrane potential (between −65 and −80 mV) and then modulated current sinusoidally around the DC level. Sinusoidal current injection produced sinusoidal modulation in membrane potential; R^2 values of sinusoidal fits to membrane potential modulation ranged from 0.87 to 0.98 (median = 0.95). We defined "subthreshold gain" at each frequency as the peak-to-peak amplitude of the best fit sine wave, normalized to the amplitude of the best fit sine wave in response to input current modulated at 0.5 Hz. "Subthreshold phase" was defined as the phase of the best fit sine wave to modulated membrane potential.

In Figure 6, the solid symbols plot subthreshold gain and phase as a function of input current frequency for a representative neuron. The frequency response of the subthreshold membrane can be described roughly as a low-pass filter. At input frequencies below about 1 Hz, both gain and phase were constant as a function of frequency. At frequencies above 1 Hz, gain declined with input frequency, while the response phase

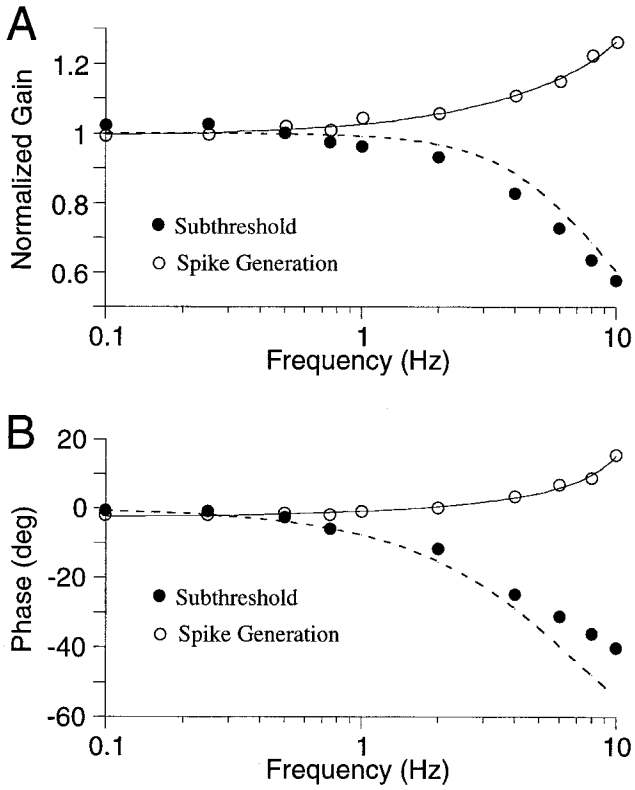

Figure 6. Comparison of the frequency response of the spike generator and that of the neuron's membrane below spike threshold. *A*, The *open symbols* plot the gain of the best sinusoidal fit to a neuron's firing rate response to sinusoidal modulation of current as a function of input frequency. Gain normalization is described in Materials and Methods. The *solid symbols* plot the normalized peak-to-peak membrane potential attained during sinusoidal modulation of injected current when the neuron hyperpolarized with DC current to a mean membrane potential of −70 mV. The *solid lines* through the *open symbols* indicate the best third order polynomial fit to the data. The *dashed lines* indicate the frequency response of an ideal low-pass filter based on an R-C circuit with a time constant of 21 msec. *B*, The *open symbols* plot the phase of the best sinusoidal fit to the firing rate response of the neuron shown in *A* to sinusoidal current modulation. The *solid symbols* plot the phase of membrane potential in response to sinusoidal modulation of injected current when the neuron was hyperpolarized with DC current.

lagged that of the input. For comparison, the dashed lines in Figure 6, *A* and *B*, indicate the gain and phase of an ideal low-pass filter with a time constant equal to the dominant time constant of the neuron, which was 21 msec. Deviations in the data from the predictions of a low-pass filter may reflect the presence of active conductances in the membrane below spike threshold (Serafin et al., 1991a,b; du Lac and Lisberger 1995).

The frequency response of the subthreshold membrane differed significantly from that of the spike generator. The open symbols in Figure 6, *A* and *B*, plot the gain and phase, respectively, of the best fit sine wave to the firing rate response to sinusoidal current modulation. At frequencies between 0.1 and 1 Hz, spike generation gain and phase were relatively constant, as were subthreshold gain and phase. However, at frequencies above 1 Hz, spike generation gain increased (Fig. 6*A*), and spike generation phase led that of input current (Fig. 6*B*).

We measured the frequency response of the subthreshold membrane in four neurons. Each neuron behaved approximately as a low-pass filter. Gain declined as a function of frequencies above 1 Hz to a mean value at 10 Hz of 0.66 (SD = 0.13).

Phase lagged that of the input by a mean value of 36° (SD = 9.5). In contrast, for neurons firing above 20 spikes/sec, spike generation gain was either constant or increased as a function of input frequency, and spike generation phase tended to lead that of the input (Fig. 5*D*). For neurons firing at mean rates of less than 20 spikes/sec, spike generation gain decreased as a function of frequency, as did subthreshold gain. However, at these firing rates spike generation gain led that of the input at frequencies greater than about 1 Hz, whereas subthreshold gain lagged that of the input at these frequencies. We conclude that the filtering properties of the membrane below spike threshold do not describe those of the spike generator.

Comparison with simple oscillator models. To gain further insight into the filtering properties of the MVN spike generator, we performed simulations of neuron-like oscillators that convert continuous current inputs into a discrete firing rate code. Our goal was to test whether the effect of mean firing rate on the frequency response of MVN neurons (Fig. 5) could be an inherent property of oscillators that encode information as modulations in firing rate. Firing rate responses to sinusoidal current injection were analyzed in two types of oscillator models, described in the Materials and Methods. Sinusoidal injection of current into both models produced sinusoidal modulations in firing rate. The models behaved linearly: firing rate responses scaled linearly as a function of input amplitude, and responses to input steps could be predicted from the Fourier synthesis of sinusoidal responses. The effects of mean firing rate on the gain and phase of firing rate responses were qualitatively similar for both models and across many variations in model parameters.

The frequency response of the oscillator models depended on mean firing rate in a manner that was similar to real MVN neurons. Figure 7 shows the frequency response of an oscillator model firing at 3 different mean rates. When the model fired at 10 spikes/sec, response gain decreased markedly as input frequency increased above 2 Hz (Fig. 7*A*). When the model fired at higher rates, response gain decreased less as a function of input frequency. The decline in gain as input frequency approaches mean firing rate reflects a smooth transition to the condition in which the input frequency equals firing rate. Under this condition, the model fired a single action potential during each cycle of the input, and firing rate was not modulated (hence response gain was zero). Response phase in the model also depended on mean firing rate, as shown in Figure 7*B*. At all firing rates, response phase led that of the input, and as input frequency increased, phase lead also increased. However, the increase in phase lead was greater for neurons firing at low mean rates than at higher mean rates (compare 10 spikes/sec with 30 spikes/sec). The trends depicted in Figure 7 were observed for both types of models and for all model parameters.

The oscillator model differed from real MVN neurons in two important ways. First, response gain in the model always declined as input frequency increased, regardless of the mean firing rate, particular model tested, or combination of model parameters. In contrast, MVN neurons firing at rates > 40 spikes/sec exhibit a gain *increase* as input frequency increases (Fig. 5). Second, the magnitude of phase leads produced by the model were substantially greater than those observed in real MVN neurons.

Discussion

Our goal was to describe the intrinsic transformations performed by medial vestibular nucleus neurons in a way that would be useful for determining how their cellular properties contribute to the processing of temporal information in VOR pathways. To assess how the spike generator in MVN neurons transforms time-varying inputs into temporal modulations of firing rate, we injected sinusoidal current intracellularly and measured the resulting pattern of action potentials. The results demonstrated that the spike generator transforms inputs into firing rates in a precise and surprisingly linear fashion over a wide range of input frequencies. Comparison of the frequency response of the spike generator with subthreshold membrane revealed that active conductances enable MVN neurons to respond well to high frequency inputs despite the low-pass characteristics of the membrane. These findings suggest that active conductances in MVN neurons play a critical role in mediating signal transformations that are appropriate for vestibulo-ocular behavior.

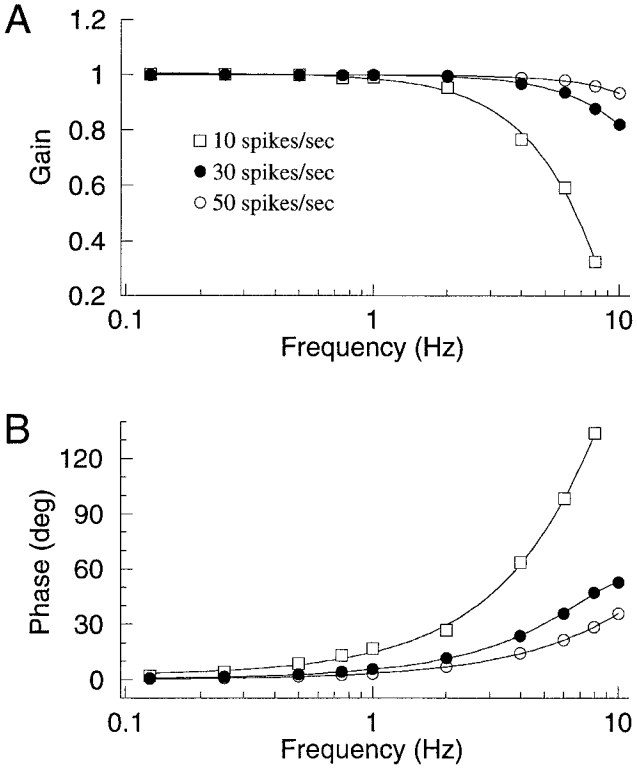

Figure 7. Frequency response of an oscillator model. In *A*, the gain of the peak-to-peak firing rate modulation, normalized as in Materials and Methods, is plotted as a function of input current frequency for a model that fired at 10 spikes/sec (*open squares*), 30 spikes/sec (*solid circles*), and 50 spikes/sec (*open circles*). In *B*, the phase of the model's firing rate response is plotted as a function of input frequency for the same firing rates as shown in *A*. Lines through the points were derived from 3rd order polynomial fits through the model data.

Assumptions

A number of assumptions must be discussed before considering possible behavioral consequences of neuronal properties that were measured *in vitro*. First, we assume that current injected intracellularly mimics synaptic current in its effect on the spike generator. The validity of this assumption has been demonstrated for steady-state inputs to motoneurons (Granit et al., 1966; Kernell, 1969; Schwindt and Calvin, 1973; Powers et al., 1992); it has not yet been tested for temporally modulated inputs. Second, we assume that the properties of the MVN spike generator that we have measured *in vitro* apply to the same neurons *in vivo*.

In awake, behaving animals, spontaneous firing rates of vestibular neurons range from 0 to over 100 spikes/sec, depending on the behavioral condition and the species. We have described the filtering properties of spike generation in neurons firing at mean rates between 10 and 70 spikes/sec; therefore, our findings apply directly to a significant subset of the range of behaviorally relevant firing rates.

Although we did not identify the synaptic inputs or projection patterns of the MVN neurons in our study, we assume that at least some of them are involved in vestibulo-ocular behavior. The MVN receives inputs from vestibular nerve afferents (Fernandez and Goldberg, 1971; Wold, 1975; Cox and Peusner, 1990) and some MVN neurons project to oculomotor nuclei (McCrea et al., 1987; Labandeira-Garcia et al., 1989; Scudder and Fuchs, 1992). A subset of MVN neurons receive monosynaptic inhibition from the cerebellar floccular lobe, a structure that participates in motor learning in the vestibulo-ocular reflex (Sato et al., 1988; du Lac and Lisberger, 1992; Lisberger et al., 1994). Although the MVN contains a variety of cell types distinguished by their synaptic connections, projection patterns, and responses during vestibulo-ocular behaviors, the intrinsic membrane and firing properties of MVN neurons are qualitatively similar when measured *in vitro* (du Lac and Lisberger, 1995).

Comparison of the transformations performed by the MVN spike generator and those required for vestibulo-ocular behavior

We have shown that MVN neurons transform input current into modulations of firing rate in a linear and precise fashion over a wide range of input frequencies. The transformations performed by MVN spike generator have a number of features in common with those performed by the neural circuitry that produces the VOR. First, the VOR circuitry transforms head movement inputs into oculomotor commands in an essentially linear fashion over a wide range of head movement amplitudes (Baarsma and Collewijn, 1974; Donaghy, 1980). Second, the behavior itself can be quite precise; many repetitions of a given head movement give rise to very reproducible eye movements. Third, the range of frequencies over which at least humans and cats experience significant head movements (from well below 1 Hz to about 7–10 Hz; Donaghy, 1980; Grossman et al., 1988), and the range of frequencies over which the VOR works well (Donaghy, 1980; Grossman et al., 1989) parallels the frequency range within which spike generation behaves linearly. These parallels suggest the possibility that the broad-band, linear filtering properties of the spike generator in MVN neurons are tailored for the requirements of vestibulo-ocular behavior.

Neural integration can not be explained by the filtering properties of the MVN spike generator. Although vestibular nerve afferents fire approximately in phase with head velocity (Fernandez and Goldberg, 1971), extraocular motoneurons carry a signal related to eye position (Skavenski and Robinson, 1973). The transformation from the head velocity signal into a position signal is thought to be accomplished by a neural form of mathematical integration (Robinson, 1989). Lesions of the medial vestibular nucleus, as well as of the neighboring prepositus nucleus, compromise the proposed integrator function (Cannon and Robinson, 1987; Cheron and Godaux, 1987). Our finding that MVN neurons are broad-band filters (rather than integrators) suggests that neural integration is mediated by synaptic transformations, dendritic filtering, and/or network mechanisms rather than by the MVN spike generator.

The finding that MVN neuronal responses to high frequency inputs depend on mean firing rate has implications for the processing of vestibular information. In the behaving animal, MVN neurons fire at low rates when the head moves rapidly and/or when the eyes are deviated in the orbit (Fuchs and Kimm, 1975; Scudder and Fuchs, 1992; Lisberger et al., 1994). Our measurements of spike generation imply that under these conditions, transmission of high frequency inputs by MVN neurons is relatively attenuated.

Processing of temporal information by the MVN spike generator

At most firing rates, the MVN spike generator can be described roughly as a broad-band linear filter: responses to high frequency inputs are equally strong as or stronger than responses to low frequency inputs. In contrast, the membrane potential below spike threshold behaves as a low-pass filter, attenuating responses to high frequency inputs. The differences between the spike generator and subthreshold membrane potential reflect the combined action of membrane conductances that are active during spike generation. These conductances shape the filtering properties of the spike generator in two qualitatively distinct ways. First, by generating action potentials they transform continuous inputs into a discrete, rate modulation code. Second, active conductances control the trajectory of the membrane potential between action potentials. Our simulations indicate that the increase in response gain at high frequencies is not an inherent feature of neuron-like oscillators that incorporate a threshold crossing mechanism to transform continuous inputs into modulations in rate. Instead, the boosting of high frequency responses must result from conductances that control the interspike membrane potential trajectory. Slow potassium conductances are likely to play a role in this process (Schwindt and Crill, 1892; Baldissera et al., 1982), but the precise filtering properties of the spike generator undoubtedly arise from the combined action of both inward and outward currents (Schwindt and Crill, 1892; Schwindt, 1992).

Our simulations of neuron-like oscillators indicate that the dependence of filtering properties on mean firing rate that we observed in MVN neurons is at least partially a consequence of rate coding. As the input frequency approaches the mean firing rate, neurons tend toward phase-locking, and the ability to signal information with modulations in firing rate becomes compromised. A hallmark of neurons in vestibulo-ocular reflex pathways, including MVN neurons, is their high spontaneous firing rates *in vivo*. The ability to robustly transmit high frequency information is apparently worth the metabolic costs incurred by high firing rates.

Spike generation in MVN neurons, when measured around a given mean firing rate, satisfies the linear requirements of scaling and additivity remarkably well. While it may be useful from the point of view of vestibulo-ocular behavior for MVN neurons to transform their inputs linearly into firing rate modulations, the fact that spike generation is linear would appear to provide a significant challenge from the point of view of the neuron. Many of the membrane conductances that comprise spike generators are themselves highly nonlinear with respect to membrane potential and time (Hille, 1992). How active, nonlinear conductances are coordinated to produce a linear spike generator in any neuron remains unknown (Schwindt, 1992).

Comparisons with spike generation in other neurons

To our knowledge, the frequency response of spike generation in vertebrate CNS neurons has been measured previously only in spinal motoneurons (Baldissera et al., 1984), and tests of additivity have not been performed previously. In motoneurons depolarized with DC current, spike generation gain and phase lead both increased as a function of input frequency, and the frequency response could be described as a first order, high-pass filter (Baldissera et al., 1984). In contrast, the frequency response of the MVN spike generator is not well-described as a simple high-pass filter at any firing rate: at low firing rates, gain decreases as frequency increases; at higher firing rates, phase is relatively constant across frequencies. Baldissera et al. (1984) reported that the frequency response of spike generation in motoneurons did not depend on mean firing rate, although they tested a limited range of firing rates compared with that reported here for MVN neurons.

Spike generation in CNS neurons has been typically measured with steps of input current. Many types of neurons increase their firing rate in an approximately linear fashion in response to steps of increasing magnitude [e.g., motoneurons (Kernell, 1965; Grantyn and Grantyn, 1978), some neocortical neurons (Staf-strom et al., 1984; Lorenzon and Foehring, 1992), brainstem auditory neurons (Manis, 1990)]. Many neuron types exhibit spike frequency adaptation, in which firing rate declines significantly over the course of an input current step [e.g., hippocampal pyramidal neurons (Madison and Nicoll, 1984), some cortical neurons (Connors and Gutnick, 1990)]. Given the assumption of linear superposition, neurons that show significant spike frequency adaptation would respond more strongly to high frequency inputs than to low frequency or steady-state inputs.

Implications for modeling

Models of neural networks commonly use "integrate and fire" units, in which changes in membrane potential that result from a combination of synaptic inputs and passive membrane properties are passed through a thresholding mechanism to produce an action potential (e.g., Worgotter and Koch, 1991; Buonomano and Mauk, 1994). Integrate and fire models are based on the assumption that a neuron's membrane time constant, measured when the neuron is below threshold for firing, determines the transformation from synaptic inputs into temporal patterns of firing. However, the present study demonstrates that spike generation in MVN neurons cannot be described as a low-pass filter; rather, the active conductances that comprise the spike generator transform the low-pass characteristics of the membrane by boosting response gain at high frequencies. As described above, in many other cell types the spike generator transmits high frequency inputs more robustly than low frequency inputs; consequently, spike generation in many CNS neurons would be better described as a high-pass filter than as the low-pass filter assumed by integrate and fire models (Schwindt 1992).

The value of models of neural systems increase when they incorporate real biological properties of neurons. Biophysically based models of neuronal function (e.g., Traub et al., 1991; McCormick and Huguenard, 1992) require many difficult measurements and can be quite computationally taxing for network models. In addition, because they are based on nonlinear membrane properties, biophysical models that describe firing rate in response to steps of inputs may not adequately describe the responses to behaviorally relevant, time-varying inputs. We suggest a simpler, biologically based alternative: quantitative descriptions of the transformation from temporally modulated current into temporal patterns of firing, such as those reported in this study, should be combined with measurements of effective synaptic current, as described by Powers et al. (1992). The result would describe completely the transformation from presynaptic firing to postsynaptic firing in a manner that is simple to compute yet based on real biological properties.

References

Baarsma EA, Collewijn H (1974) Vestibulo-ocular and optokinetic reactions to rotation and their interactions in the rabbit. J Physiol (Lond) 238:603–625.

Baldissera F, Campadelli P, Piccinelli L (1982) Neural encoding of input transients investigated by intracellular injection of ramp currents in cat alpha-motoneurones. J Physiol (Lond) 328:73–86.

Baldissera F, Campadelli P, Piccinelli L (1984) The dynamic response of cat alpha-motoneurones investigated by intracellular injection of sinusoidal currents. Exp Brain Res 54:275–282.

Bracewell RB (1986) The Fourier transform and its applications. New York: McGraw-Hill.

Buonomano DV, Mauk MD (1994) Neural network model of the cerebellum: temporal discrimination and the timing of motor responses. Neural Comput 6:38–55.

Cannon SC, Robinson DA (1987) Loss of the neural integrator of the oculomotor system from brain stem lesions in monkey. J Neurophysiol 57:1383–1409.

Cheron G, Godaux E (1987) Disabling of the oculomotor neural integrator by kainic acid injections in the prepositus-vestibular complex of the cat. J Physiol (Lond) 394:267–290.

Chubb MC, Fuchs AF, Scudder CA (1984) Neuronal activity in monkey vestibular nuclei during vertical vestibular stimulation and eye movements. J Neurophysiol 52:724–742.

Collewijn H, Grootendorst AF (1978) Adaptation of the rabbit's vestibulo-ocular reflex to modified visual input: importance of stimulus conditions. Arch Ital Biol 116:273–280.

Connors BW, Gutnick MJ (1990) Intrinsic firing patterns of diverse neocortical neurons. Trends Neurosci 13:99–104.

Cox R, Peusner K (1990) Horseradish peroxidase labelling of the central pathways in the medulla of the ampullary nerves in the chicken, *Gallus gallus*. J Comp Neurol 297:564–585.

Cullen KE, McCrea RA (1993) Firing behavior of brain stem neurons during voluntary cancellation of the horizontal vestibuloocular reflex. I. Secondary vestibular neurons. J Neurophysiol 70:828–843.

Cullen KE, Chen-Huang C, McCrea RA (1993) Firing behavior of brain stem neurons during voluntary cancellation of the horizontal vestibuloocular reflex. II. Eye movement related neurons. J Neurophysiol 70:844–856.

Donaghy M (1980) The cat's vestibulo-ocular reflex. J Physiol (Lond) 300:337–351.

du Lac S, Lisberger SG (1992) Eye movements and brainstem neuronal responses evoked by cerebellar and vestibular stimulation in chicks. J Comp Physiol A 171:629–638.

du Lac S, Lisberger SG (1995) Membrane and firing properties of avian medial vestibular nucleus neurons *in vitro*. J Comp Physiol A 176:641–651.

Fernandez C, Goldberg J (1971) Physiology of peripheral neurons innervating semicircular canals of the squirrel monkey. II. Response to sinusoidal stimulation and dynamics of peripheral vestibular system. J Neurophysiol 34:661–675.

Fuchs AF, Kimm J (1975) Unit activity in the vestibular nucleus of the alert monkey during horizontal angular acceleration and eye movement. J Neurophysiol 38:1140–1161.

Gonshor A, Melvill-Jones G (1976) Extreme vestibulo-ocular adaptation induced by prolonged optical reversal of vision. J Physiol (Lond) 256:381–414.

Granit R, Kernell D, Lamarre Y (1966) Algebraic summation in synaptic activation of motoneurones firing within the 'primary range' to injected currents. J Physiol 187:379–399.

Grantyn R, Grantyn A (1978) Morphological and electrophysiological properties of cat abducens motoneurons. Exp Brain Res 31:249–274.

Grossman GE, Leigh RJ, Abel LA, Lanska DJ, Thurston SE (1988)

Frequency and velocity of rotational head perturbations during locomotion. Exp Brain Res 70:470–476.
Grossman GE, Leigh RJ, Bruce EN, Huebner WP, Lanska DJ (1989) Performance of the human vestibuloocular reflex during locomotion. J Neurophysiol 62:264–272.
Hille B (1992) Ionic channels of excitable membranes. Sunderland, MA: Sinauer.
Ito M, Shiida T, Yagi N, Yamamoto M (1974) The cerebellar modification of rabbit's horizontal vestibulo-ocular reflex induced by sustained head rotation combined with visual stimulation. Proc Jpn Acad 50:85–89.
Keller EL (1978) Gain of the vestibulo-ocular reflex in monkey at high rotational frequencies. Vision Res 18:311–315.
Kernell D (1965) The adaptation and relation between discharge frequency and current strength of cat lumbrosacral motoneurones stimulated by long-lasting current. Acta Physiol Scand 65:65–73.
Kernell D (1969) Synaptic conductance changes and the repetitive impulse discharge of spinal motoneurons. Brain Res 15:291–294.
Labandeira-Garcia JL, Guerra-Seijas MJ, Labandeira-Garcia JA, Suarez-Nunez JM (1989) Afferent connections of the oculomotor nucleus in the chick. J Comp Neurol 282:523–534.
Lisberger SG, Miles FA (1980) Role of primate medial vestibular nucleus in adaptive plasticity of vestibulo-ocular reflex. J Neurophysiol 43:1725–1745.
Lisberger SG, Pavelko TA, Broussard DM (1994a) Neural basis for motor learning in the vestibulo-ocular reflex of primates. I. Changes in the responses of brainstem neurons. J Neurophysiol 72:928–953.
Lisberger SG, Pavelko TA, Broussard DM (1994b) Responses during eye movements of brainstem neurons that receive monosynaptic inhibition from the flocculus and ventral paraflocculus in monkeys. J Neurophysiol 72:909–928.
Lorenzon NM, Foehring RC (1992) Relationship between repetitive firing and afterhyperpolarizations in human neocortical neurons. J Neurophysiol 67:350–363.
Madison DV, Nicoll RA (1984) Control of the repetitive discharge of rat CA1 pyramidal neurones *in vitro*. J Physiol (Lond) 354:319–331.
Manis PB (1990) Membrane properties and discharge characteristics of guinea pig dorsal cochlear nucleus neurons studied *in vitro*. J Neurosci 10:2338–2351.
McCormick DA, Huguenard JR (1992) A model of the electrophysiological properties of thalamocortical relay neurons. J Neurophysiol 68:1384–1400.
McCrea RA, Strassman A, May E, Highstein SM (1987a) Anatomical and physiological characteristics of vestibular neurons mediating the horizontal vestibulo-ocular reflex of the squirrel monkey. J Comp Neurol 264:547–570.
McCrea RA, Strassman A, May E, Highstein SM (1987b) Anatomical and physiological characteristics of vestibular neurons mediating the vertical vestibulo-ocular reflex of the squirrel monkey. J Comp Neurol 264:571–594.
McFarland JL, Fuchs AF (1992) Discharge patterns of the nucleus prepositus and adjacent medial vestibular nucleus during horizontal eye movements in behaving monkeys. J Neurophysiol 68:319–332.
Melvill-Jones G (1977) Plasticity in the adult vestibulo-ocular reflex arc. Philos Trans R Soc Lond [Biol] 278:319–334.
Miles FA, Eighmy BB (1980) Long-term adaptive changes in primate vestibulo-ocular reflex. I. Behavioral observations. J Neurophysiol 43:1406–1425.
Ohgaki T, Curthoys IS, Markham CH (1988) Morphology of physiologically identified second-order vestibular neurons in cat, with intracellularly injected HRP. J Comp Neurol 276:387–411.
Powers RK, Robinson FR, Konodi MA, Binder MD (1992) Effective synaptic current can be estimated from measurements of neuronal discharge. J Neurophysiol 68:964–968.
Robinson DA (1989) Integrating with neurons. Annu Rev Neurosci 12: 33–45.
Sato Y, Kanda K-I, Kawasaki T (1988) Target neurons of floccular middle zone inhibition in medial vestibular nucleus. Brain Res 446: 225–235.
Schairer JO, Bennett MVL (1986) Changes in the gain of the vestibulo-ocular reflex by combined visual and vestibular stimulation in goldfish. Brain Res 373:164–176.
Schwindt PC (1992) Ionic currents governing input-output relations of Betz cells. In: Single neuron computation (Davis J, ed), pp 235–258.
Schwindt PC, Calvin WH (1973) Equivalence of synaptic and injected current in determining the membrane potential trajectory during motoneuron rhythmic firing. Brain Res 59:389–394.
Schwindt PC, Crill WE (1892) Factors influencing motoneuron rhythmic firing: results from a voltage clamp study. J Neurophysiol 48: 875–889.
Scudder CA, Fuchs AF (1992) Physiological and behavioral identification of vestibular nucleus neurons mediating the horizontal vestibuloocular reflex in trained rhesus monkeys. J Neurophysiol 68:244–264.
Serafin M, Waele Cd, Khateb A, Vidal PP, Muhlethaler M (1991a) Medial vestibular nucleus in the guinea-pig. I. Intrinsic membrane properties in brainstem slices. Exp Brain Res 84:417–425.
Serafin M, Waele Cd, Khateb A, Vidal PP, Muhlethaler M (1991b) Medial vestibular nucleus in the guinea-pig. II. Ionic basis of the intrinsic membrane properties in brainstem slices. Exp Brain Res 84: 426–433.
Skavenski AA, Robinson DA (1973) Role of abducens neurons in vestibuloocular reflex. J Neurophysiol 36:724–738.
Snyder LH, King WM (1992) Effect of viewing distance and location on the axis of head rotation on the monkey's vestibuloocular reflex. I. Eye movement responses. J Neurophysiol 67:861–874.
Stafstrom CE, Schwindt PC, Crill WE (1984) Repetitive firing in layer V neurons from cat neocortex *in vitro*. J Neurophysiol 52:264–277.
Tomlinson RD, Robinson DA (1984) Signals in vestibular nucleus mediating vertical eye movements in the monkey. J Neurophysiol 51: 1121–1136.
Traub RD, Wong RKS, Miles R, Michelson H (1991) A model of a CA3 hippocampal pyramidal neuron incorporating voltage-clamp data on intrinsic conductances. J Neurophysiol 66:635–650.
Wallman J, Velez J, Weinstein B, Green A (1982) Avian vestibulo-ocular reflex: adaptive plasticity and developmental changes. J Neurophysiol 48:952–967.
Wold JE (1975) The vestibular nuclei in the domestic hen (*Gallus domesticus*). II. Primary afferents. Brain Res 95:531–543.
Worgotter F, Koch C (1991) A detailed model of the primary visual pathway in the cat: comparison of afferent excitatory and intracortical inhibitory connection schemes for orientation selectivity. J Neurosci 11:1959–1979.